Aerosol and Air Quality Research, 16: 1541–1547, 2016

ISSN: 1680-8584 print / 2071-1409 online
doi: 10.4209/aaqr.2015.10.0586

Effective Coagulation Coefficient Approach for Estimating Particle Number Emission Rates for Strong Emission Sources

Srinivasan Anand[1], Bathula Sreekanth[2], Yelia Shankaranarayana Mayya[3*]

[1] *Health Physics Division, Bhabha Atomic Research Centre, Trombay, Mumbai 400085, India*
[2] *Radiation Safety Systems Division, Bhabha Atomic Research Centre, Trombay, Mumbai 400085, India*
[3] *Department of Chemical Engineering, Indian Institute of Technology Bombay, Mumbai 400076, India*

ABSTRACT

Particle number emission rate is one of the important parameters that characterizes the emission source and it is an essential input to the aerosol dynamics models. Estimation of this quantity at the source is rather complicated due to the combined action of ventilation and coagulation on the depletion of particle number concentrations. Techniques to estimate number emission rate are still at preliminary stage and hence there is a definite need to develop a methodology for this purpose. In the present study, an effective coagulation coefficient (K_{eff}) approach is provided to correct for coagulation losses encountered during experiments for the determination of number emission rate. K_{eff} is expressed as a function of single parameter (β) namely the ratio of the prescribed ventilation rate and measured number concentration in the experiments. The utility of the approach is demonstrated by applying it to few practical cases reported in the literature. The results are further discussed.

Keywords: Coagulation; Ventilation; Emission rate; Number concentration; Aerosols.

INTRODUCTION

Emission of Ultra-fine particles (UFPs) due to combustion, gas-to-particle conversion and vapour phase nucleation are of increasing concern in the context of air pollution, climate change and health effects. Industrial emissions, biomass burning, material synthesis and engineered nanoparticles are some of the human activities responsible for these emissions. Mass and number emission rates are two important parameters that characterise these sources. Several techniques have been implemented for assessing mass emission factor which is primarily defined as the mass of aerosol (g) emitted per unit mass of the fuel combusted (kg). From the knowledge of the combustion rate of the fuel (kg s^{-1}), and the volume (m^3) into which the aerosol is dispersed, one can estimate respectively the mass emission rate (g s^{-1}) or the mass emission rate density (g s^{-1} m^{-3}). One of the most common methods of estimating mass emission factors is to inject particles from a specified mass of the source into a well-ventilated chamber, measure the mass concentration of the aerosol and apply steady-state mass balancing calculations. In addition to mass, particle number concentrations and number emission rates from combustion sources are emerging as important ultrafine particle metrics in inhalation toxicology (Bhangar *et al.*, 2011; Dhaniyala *et al.*, 2011). While mass emission factors for the case of biomass burning are well established (Reddy and Venkataraman, 2002), techniques to estimate number emission factors are still at a preliminary state because of the difficulties associated with near-source monitoring and the effect of coagulation. It is not a simple matter to quantify the number concentration very near to the strong emission sources due to higher temperatures and also the number concentrations that are likely to attain upper limiting value of the particle counters. On the other hand, measurements away from the source location lead to rapid decrease in number concentration due to coagulation.

To circumvent the problem of coagulation, Kittelson (1998, 2001) developed dilution based techniques for estimating the number emission rates in the context of diesel particle emissions from vehicular exhausts. In the context of indoor sources, large dilution may not always be possible and some studies either ignore the coagulation loss (Wallace *et al.*, 2004; Wallace and Ott, 2011) or treat it as a linear removal process (Bhangar *et al.*, 2011) to simplify the emission rate estimations. Although Wallace *et al.* (2008) observed the importance of coagulation in their experiments they did not provide an approach to estimate coagulation-corrected emission rates for strong sources. Hussein *et al.* (2005) estimated emission rates in an iterated manner based on the difference between measurements

* Corresponding author.
Tel.: +91-22-25767228
E-mail address: ysmayya@iitb.ac.in

and model simulation results. Anand *et al.* (2014) proposed a potentially useful property of scaling behaviour for estimating number emission rates in the absence of, or the presence of weak ventilation. All these studies show the complicated effects of coagulation and ventilation processes that rapidly alter the number-size spectrum as one moves away from the source rendering it difficult to relate them to the number emission rate at the source. There is thus, a fundamental need to develop a reliable method to account for coagulation effects for estimating number emission rates. In the present work, a simple "effective coagulation coefficient" approach is provided to correct for coagulation losses based on the maintained ventilation rate and measured number concentration in dilution chamber experiments.

METHODS

We examine the dynamics and fate of particles emitted from a continuous, steady source in the presence of coagulation, ventilation and wall depositions (Fig. 1). Most of the source emission rate estimation methods (Mitra *et al.*, 2002; Wallace *et al.*, 2004; Mullen *et al.*, 2011) use the concept of mass balance between generation and ventilation removal of the monitored number/mass concentration-size spectrum data. Quite often, this procedure may not be adequate for strong sources such as that due to combustion unless the joint effect of coagulation and ventilation is properly addressed. This requires development of a detailed numerical solution for the spectral evolution of the aerosol size distribution by considering the Fuchs coagulation kernel that incorporates Brownian diffusion effects over the entire particle size range. Main difficulty in applying coagulation corrections pertains to the intricate size dependent nature of Fuchs kernel. However, in a practical context, it may not be always possible to perform numerical simulations of the coagulation process to estimate the source strength from the measured data. It is more helpful to provide a simple recipe by an analytically tractable solution of the coagulation equation for a size-independent "effective" coagulation coefficient. With this in view, we propose an "effective coagulation coefficient" which captures the spectrally averaged Fuchs kernel for different ventilation rates and source strengths. Since it is now size independent, one can easily relate it to the strength of the source through the measured steady-state concentration and ventilation rate by the well-known constant kernel solution with ventilation, given below:

$$S = 0.5K_{eff}(N_0, \lambda)N_0^2 + \lambda N_0 \quad (1)$$

where, S is size-integrated source emission rate, K_{eff} is effective coagulation coefficient, $\lambda = \lambda_w + \lambda_v$ is effective removal rate, λ_w is total wall loss rate independent of particle size, λ_v is ventilation removal rate, and N_0 is steady-state total number concentration. The source strength can then be easily estimated from Eq. (1), providing the dependency of K_{eff} on source and ventilation parameters, is explicitly known.

To develop this dependency, we note that a satisfactory representation of the effective coagulation coefficient should take into account hetero-coagulation effects across the entire steady-state size spectrum. This is best accomplished by averaging Fuchs coagulation kernel ($K_{Fuchs}(u, v)$) incorporating Brownian diffusion effects over the steady-state number spectrum $n(u)n(v)dudv$ as follows:

$$K_{eff}\left(N_0, \lambda\right) = \frac{\int_{u_0}^{\infty}\int_{u_0}^{\infty} K_{Fuchs}(u,v)\, n(u, N_0, \lambda)\, n(v, N_0, \lambda)\, du\, dv}{N_0^{\,2}} \quad (2)$$

where, $K_{Fuchs}(u, v)$ is the coagulation kernel by Fuchs and u_0 is the primary particle size which is lower end of the size spectrum. Assuming a constant coagulation kernel, solution to the coagulation equation with a steady source and removal rates were first provided by Hendriks and Ziff (1985). However, these solutions obtained by generating functions techniques for the discrete version of the coagulation

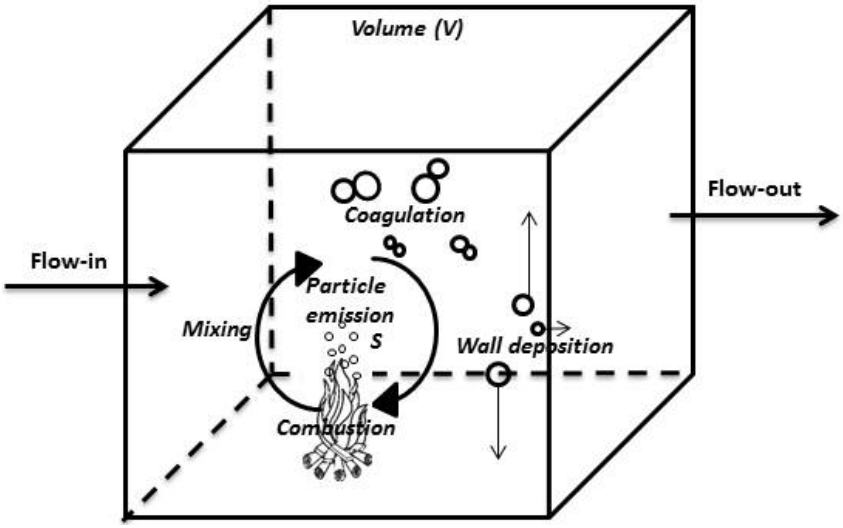

Fig. 1. Schematic diagram - aerosol microphysical processes in the study volume.

equation, are not readily adaptable for our purpose. In the present study, we have used Laplace Transform method to obtain a continuum form of the solution as shown in the Appendix. The integral in Eq. (2) is then evaluated using this solution (Eq. (A14)):

$$n(u)du = \frac{N_0}{\gamma^{1/2}\Gamma(-1/2,\gamma)}\left(\frac{u}{u_0}\right)^{-3/2} e^{-\gamma\frac{u}{u_0}}\frac{du}{u_0} \tag{3}$$

where, the concentration distribution $n(u)$ now depends on the system variables through a parameter γ, defined as

$$\gamma = \ln\left[1+\frac{\beta^2}{K_{eff}^2+2\beta K_{eff}}\right]. \tag{4}$$

β is defined as λ_{total}/N_0 ($m^3\ s^{-1}$), and it captures the two important basic parameters in the model, viz., total removal rate and steady-state number concentration, in a single term. If we define a variable $x = u/u_0$, then Eq. (3) becomes,

$$f(x;\gamma) = \frac{n(u)u_0}{N_0} = \frac{x^{-3/2}e^{-\gamma x}}{\gamma^{1/2}\Gamma(-1/2,\gamma)} \tag{5}$$

Substituting Eq. (5) in Eq. (2), we get

$$K_{eff}(u_0,\gamma) = \frac{1}{\left[\gamma^{1/2}\Gamma(-1/2,\gamma)\right]^2}\int_1^\infty\int_1^\infty K_{Fuchs}(u_0x,u_0y)(xy)^{-3/2}e^{-\gamma(x+y)}dxdy \tag{6}$$

Eqs. (4)–(6) show that the effects of N_0 and λ on K_{eff} are captured through a single parameter $\beta = \lambda/N_0$ for a given u_0, which greatly simplifies the graphical representation of the effective coagulation coefficient. Since Eqs. (4)–(6) are coupled nonlinearly, they are solved iteratively for a given β until K_{eff} converges to an accurate value, by evaluating the double integral with the help of Mathematica (Wolfram Inc., 2005). To illustrate this approach, an initial particle diameter (d_{p0}) of 10 nm is chosen which is generally ascribed as the Count Median Diameter (CMD) to the source particles for fuels such as gas and kerosene (Wallace *et al.*, 2008). Since most measurements of particle sizes correspond to post coagulation scenario (measured few meters away), they are expected to be larger than the original primary particle sizes near the source. The results may not be very sensitive to the choice of primary particle size around 10 nm. For example, our calculations indicate that for a choice of d_{p0} = 20 nm, the self-coagulation coefficient differs by about ~20% and the effect on steady-state concentration is less than 10% as compared to the case of d_{p0} = 10 nm. In applying Fuchs kernel, we also assume compact particles having fractal dimension (d_f) of 3.

Fig. 2 shows the plot of variation of K_{eff} w.r.t β, for u_0 corresponding 10 nm diameter and for d_f = 3. One can develop similar plots for situations of widely differing values of d_f and u_0, using the nonlinear prescription setup in Eq. (6). The K_{eff} thus obtained asymptotically approaches a lowest value of 2×10^{-15} $m^3\ s^{-1}$ for large β and increases to about 5.5×10^{-15} $m^3\ s^{-1}$ as $\beta \to 0$, displaying variability by more than a factor of 2. The domain of large β (say, $> 20 \times 10^{-16}$ $m^3 s^{-1}$) corresponds to either large ventilation or weak sources and hence coagulation corrections using Eq. (1) will be negligible. As β decreases, coagulation correction becomes progressively more important and Eq. (1) combined with Fig. 2 provides a simple and theoretically consistent recipe to evaluate the source strength. The following empirical fit in terms of a logistic function to the graph equally serves a convenient representation of K_{eff} for practical purposes:

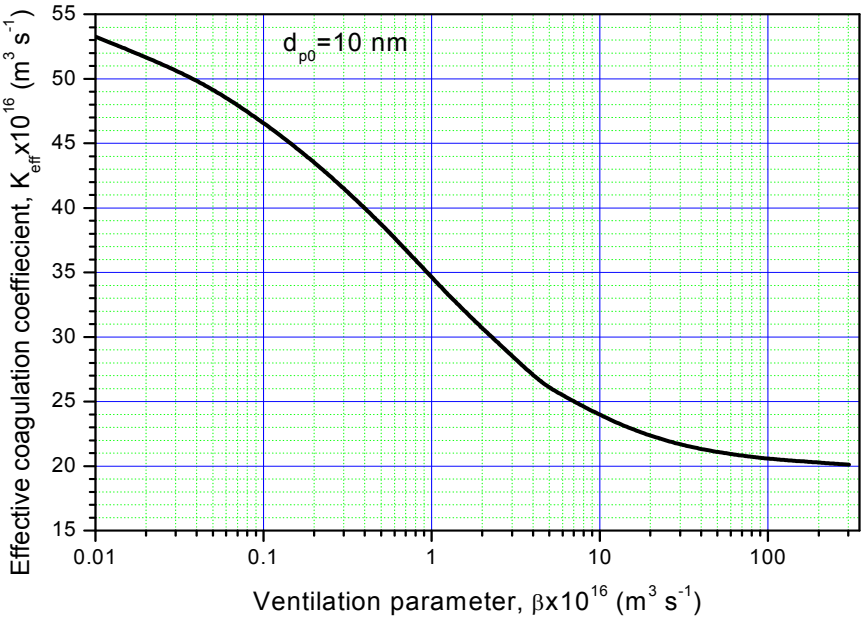

Fig. 2. Effective coagulation kernel (K_{eff}) computed for an initial particle diameter (d_{p0}) of 10 nm using Eqs. (4)–(6).

$$K_{eff}(m^3 s^{-1}) = 10^{-16}\left[19.44 + \frac{35.31}{1+\left(\frac{10^{16}\beta(m^3 s^{-1})}{0.64}\right)^{0.689}}\right] \quad (7)$$

RESULTS AND DISCUSSION

The method described in the previous section has been applied to some of the reported studies for obtaining the coagulation corrected number emission rates. The results are tabulated in Table 1. The first case is an internal consistency check with our numerical simulation data itself. We consider the scenario in which nanoparticles are released continuously into a large indoor volume, and the aerosol system evolves by continuous injection of particles at a constant rate, by coagulation, and by removal/dilution with clean air at a constant rate. If the aerosol is mixed rapidly through mixing elements such as fans or induced ventilation, one may, to a first approximation, treat the aerosol concentration as spatially homogeneous at all times. Then the rate of change of aerosol concentration in the chamber is given by

$$\frac{\partial n(u,t)}{\partial t} = S(u,t) + \frac{1}{2}\int_0^u K(u', u-u')\, n(u',t)\, n(u-u',t)\, du' - n(u,t)\int_0^\infty K(u',u)\, n(u',t)\, du' - \{\lambda_v + \lambda_w(u)\}\, n(u,t) \quad (8)$$

where, $n(u, t)$ is the number of particles with volumes lying between u and $u + du$ per unit volume of the fluid at time t (m^{-3} μm^{-3}), $\lambda_w(u)$ is the size-dependent removal rate due to wall/surface deposition processes (Lai and Nazaroff, 2000), $S(u, t) = (\dot{V}_s/V)Q(u, t)$ is the particle number injection rate distribution of the source (m^{-3} μm^{-3} s^{-1}) defined as the mean number of particles injected per unit volume of space per unit time per unit particle volume around u, $\dot{V}_s$ is the source volume flow rate to the chamber (m^3 s^{-1}), V is the volume of the chamber (m^3), and $Q(u, t)$ is the number concentration distribution at the source (m^{-3} μm^{-3}). The initial number concentration distribution in the chamber is assumed to be zero ($n(u, 0) = 0$). The first term in the RHS of Eq. (8) represent continuous source injection, the second and third terms represent coagulation, and the fourth for ventilation and size dependent removal processes. Eq. (8) is numerically solved using nodal method combined with finite difference scheme (Anand and Mayya, 2009; Anand *et al.*, 2012) to obtain the steady-state number concentration with the following input parameters: $S = 10^{11}$ # m^{-3} sec^{-1}, CMD = 10 nm, GSD = 1.3, $\lambda_v = 0.5$ h^{-1}. It is found that the estimate of the particle number emission rate (S) obtained from the K_{eff} method is about 13% higher than S_{true} value chosen for the numerical simulation. This is expected since a constant kernel, however well weighted it is, can not exactly capture the nuances of a size dependent kernel such as the Fuchs kernel. This difference also indicates the inevitable level of error expected from the use of this method. In Fig. 3, we have compared the steady-state size spectrum of constant kernel (K_{eff}) method with that of numerical simulation using size-dependent Fuchs kernel. It is seen that beyond $u/u_0 > 1$, the two curves show a similar decrease in the concentration distribution with respect to particle size (Fig. 3). However, the slight shift is expectedly due to the error in the estimation of number emission rate (S) as described above.

The second case corresponds to the study of Wallace *et al.* (2008) for a combustion source in an uninhabited house, and we find that the estimate based on the present K_{eff} method is ~25 times higher than the value reported by the authors. From the reported λ and N_0 data, the β estimate for this case turns out to be about 10^{-16} $m^3 s^{-1}$ and from the discussions in the previous section, this corresponds to the region of dominance of coagulation over removal. Thus coagulation correction leads to a significant change in the emission rate estimate. The third case study is from Afshari *et al.* (2005) that involved several experiments conducted in a 32 m^3 study volume with different emission sources using candle and cigarettes. The β parameter estimate for this case is large ($> 20 \times 10^{-16}$ $m^3 s^{-1}$) and this corresponds to a situation where coagulation correction is negligible. This fact is supported by the excellent agreement seen between the estimates from the present method with the reported values. Similar is the situation in the last case study (Mullen *et al.*, 2011), although we are unable to make a comparison as the authors have not provided number emission rate estimates. These comparisons clearly demonstrate usefulness of the K_{eff} method for estimating coagulation corrected

Table 1. Comparison of source emission rates for different emission scenario.

Removal rate, h^{-1}		N_0, # m^{-3}	λ/N_0, m^3 s^{-1}	Integral method		Reported source emission rate, m^{-3} s^{-1}	Reference
λ_v	λ_w			K_{eff}, m^3 s^{-1}	S, m^{-3} s^{-1}		
0.5	0.45	7.4×10^{12}	3.6×10^{-17}	4.05×10^{-15}	1.13×10^{11}	1×10^{11}	Present study
0.23	0.45	$\sim 2 \times 10^{12}$	9.44×10^{-17}	3.47×10^{-15}	7.32×10^{9}	$0.29 \times 10^{9*}$	Wallace *et al.*, 2008
1.7	0.3	2.41×10^{11}	2.31×10^{-15}	2.2×10^{-15}	2×10^{8}	$1.9 \times 10^{8\$}$	- Wax candle$^{\$}$
		2.13×10^{11}	2.61×10^{-15}	2.2×10^{-15}	1.7×10^{8}	$1.96 \times 10^{8\$}$	- Cigarette$^{\$}$
0.5	1.0	2.0×10^{10}	2.1×10^{-14}	2.0×10^{-15}	8.7×10^{6}	-	Mullen *et al.*, 2011
3.2	1.0	2.0×10^{10}	5.8×10^{-14}	1.98×10^{-15}	2.4×10^{7}		

* - based on author's estimate of 6×10^{12} # min^{-1} release rate and 340 m^3 study volume.

$ - based on author's estimate of 3.65×10^{11} # min^{-1} and 3.76×10^{11} # min^{-1} release rate for candle and cigarette sources respectively in 32 m^3 study volume from Afshari *et al.* (2005).

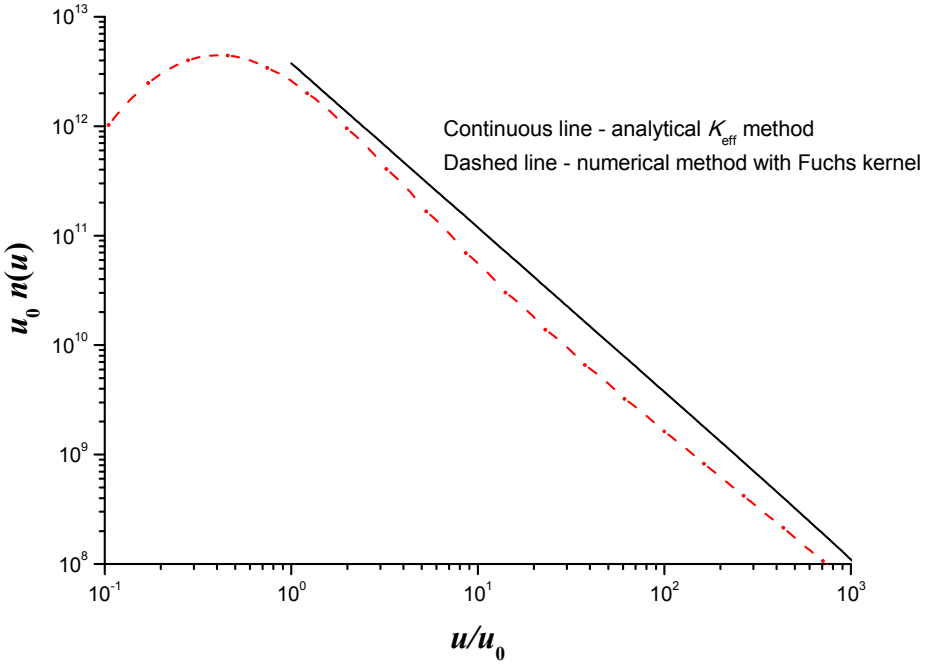

Fig. 3. Steady-state number size distributions for a typical aerosol system ($S = 10^{11}$ m^{-3} s^{-1}) for (i) constant kernel (K_{eff}) solution (Eq. (3)) with $d_{p0} = 10$ nm, and (ii) numerical solution using Fuchs kernel (CMD = 10 nm; GSD – 1.3).

number emission rates for sources using total removal rate and steady-state number concentration obtained from the experiments.

CONCLUSIONS

The present study provides an effective coagulation coefficient approach to correct for coagulation effect in experiments for estimating the number emission rates from strong sources. This approach requires few measured parameters such as number concentration and removal rate. In addition to this, a simple fitting formula using the realistic Fuchs coagulation kernel is presented to calculate effective coagulation coefficient. Applications to few practical problems show that this method is simple and efficient tool to estimate number emission rate at the source.

Appendix - Derivation of Steady-State Size Distribution for Ventilation-Coagulation Problem with Constant Kernel

The rate of change of number concentration in an aerosol system with steady generation rate of particles and steady removal rate is given by,

$$\frac{\partial n(u,t)}{\partial t} = \frac{1}{2}\int_0^u K(u', u-u')n(u',t)n(u-u',t)du' - n(u,t)\int_0^\infty K(u,u')n(u',t)du' - \lambda n(u,t) + S(u,t) \quad \text{(A1)}$$

where the variables are same as that defined in the main text. We assume that the source generation rate distribution density (m^{-3} μm^{-3} s^{-1}) produces primary particles of size u_0 only. i.e.,

$$S(u, t) = S_0\, \delta(u - u_0) \quad \text{(A2)}$$

where, S_0 is the total number of particles produce per second. Once there is a steady source and removal, we assume that there will be a steady-state size spectrum. Further, assuming constant kernel ($K(u, u') = K_{eff}$), Eq. (A1) reduces to an integral equation for the steady-state number size distribution function:

$$\frac{K_{eff}}{2}\int_0^u n(u')n(u-u')du' - K_{eff}\, n(u)N_0 - \lambda n(u) + S_0\delta(u-u_0) = 0 \quad \text{(A3)}$$

where, K_{eff} is the effective coagulation coefficient (m^3 s^{-1}) and N_0 is the total (size-integrated) particle number concentration (m^{-3}). The Laplace transform of Eq. (A3) w.r.t u variable:

$$\frac{K_{eff}}{2}\tilde{n}(p)^2 - \left\{K_{eff}N_0 + \lambda\right\}\tilde{n}(p) + S_0 e^{-pu_0} = 0 \quad \text{(A4)}$$

where, $\tilde{n}(p) \equiv \int_0^\infty e^{-pu} n(u)du$, and p is conjugate to u. We also make use of convolution theorem of Laplace transform for the first term of Eq. (A3). If we now set $p = 0$ in Eq. (A4) and rearrange the resultant equation for the total number concentration ($\tilde{n}(0) = N_0$), we get

$$S_0 = \frac{K_{eff}}{2} N_0^{\,2} + \lambda N_0 \tag{A5}$$

The physically admissible solution to the quadratic equation (Eq. (A4)) is,

$$\tilde{n}(p) = b\left[1 - \sqrt{1 - \frac{2ce^{-pu_0}}{b^2}}\right] \tag{A6}$$

where, $b = \frac{K_{eff} N_0 + \lambda}{K_{eff}}$ and $c = \frac{S_0}{K_{eff}}$.

To Laplace invert Eq. (A6) we can expand the under-root term using binomial theorem which will yield the following series:

$$1 - \left(1 - x\right)^{1/2} = \frac{1}{2\sqrt{\pi}} \sum_{n=1}^{\infty} \frac{\left(n - 3/2\right)\,!}{n\,!} x^n \tag{A7}$$

That is, Eq. (A6) can be rewritten as,

$$\tilde{n}(p) = \frac{b}{2\sqrt{\pi}} \sum_{n=1}^{\infty} \left[\frac{\left(n - 3/2\right)\,!}{n\,!} \left(\frac{2c}{b^2}\right)^n e^{-npu_0}\right] \tag{A8}$$

Inverse Laplace Transform of Eq. (A8) becomes

$$n(u) = \frac{b}{2\sqrt{\pi}} \sum_{n=1}^{\infty} \left[\frac{\left(n - 3/2\right)\,!}{n\,!} \left(\frac{2c}{b^2}\right)^n \delta(u - nu_0)\right] \tag{A9}$$

Eq. (A9) is the exact solution for the steady-state particle volume distribution, which is a series of delta functions w.r.t integer multiples of source particle volume. The n-dependent coefficients of delta function terms give the intensity of occurrence of a size $u = nu_0$. To express it in terms of a continuous distribution function, we replace "$n = u/u_0$" in the coefficient of the delta function and use sterling approximation ($n\,! \sim \sqrt{2\pi\, n}.n^n \exp(-n)$) for all the factorial expressions. Hence,

$$\frac{\left(n - 3/2\right)\,!}{n\,!} \sim \left(\frac{u}{u_0}\right)^{-3/2} \text{ and } \left(\frac{2c}{b^2}\right)^n = e^{-\ln\left(b^2/2c\right)\frac{u}{u_0}} = e^{-\gamma\frac{u}{u_0}} \tag{A10}$$

where,

$$\gamma \equiv \ln\left(\frac{b^2}{2c}\right) = \ln\left[\frac{\left(K_{eff} N_0 + \lambda\right)^2}{2K_{eff} S_0}\right] = \ln\left[1 + \frac{\beta^2}{K_{eff}^2 + 2\beta K_{eff}}\right],$$

and $\beta = \lambda/N_0$.

Then, the continuum equivalent of Eq. (A9) will be

$$n(u) = A\left(\frac{u}{u_0}\right)^{-3/2} e^{-\ln\left(b^2/2c\right)\frac{u}{u_0}}, \text{ for } u > u_0. \tag{A11}$$

where, A is a normalization constant, which cannot be obtained from the series, but have to be determined from the integral using the fact that

$$N_0 = \int_{u_0}^{\infty} n(u)du = A\int_{u_0}^{\infty} \left(\frac{u}{u_0}\right)^{-3/2} e^{-\gamma\frac{u}{u_0}} du = Au_0\gamma^{1/2} \int_{\gamma}^{\infty} y^{-3/2} e^{-y} dy \tag{A12}$$

Therefore,

$$A = \frac{N_0}{u_0\gamma^{1/2} \int_{\gamma}^{\infty} y^{-3/2} e^{-y} dy} = \frac{N_0}{u_0\gamma^{1/2}\Gamma\left(-1/2, \gamma\right)} \tag{A13}$$

where, $\Gamma(-1/2, \gamma)$ is incomplete gamma function defined by the integral in the denominator. By substituting Eq. (A13) in Eq. (A11), we get the required solution for the steady-state size distribution,

$$n(u)du = \frac{N_0}{\gamma^{1/2}\Gamma(-1/2, \gamma)} \left(\frac{u}{u_0}\right)^{-3/2} e^{-\gamma\frac{u}{u_0}} \frac{du}{u_0}. \tag{A14}$$

REFERENCES

Afshari, A., Matson, U. and Ekberg, L.E. (2005). Characterization of indoor sources of fine and ultrafine particles: a study conducted in a full-scale chamber. *Indoor Air* 15: 141–150.

Anand, S., Joshi, M., Sapra, B.K. and Mayya, Y.S. (2014). Estimating number emission rates of nano-particle sources by "Concentration Peaking" method. Aerosol Technology 2014, Karlsruhe, Germany, Abstract T220A02.

Anand, S. and Mayya, Y.S. (2009). Coagulation in a diffusing Gaussian aerosol puff: Comparison of analytical approximations with numerical solutions. *J. Aerosol Sci.* 40: 348–361.

Anand, S., Mayya, Y.S., Yu, M., Seipenbusch, M. and Kasper, G. (2012). A numerical study of coagulation of nanoparticle aerosols injected continuously into a large, well stirred chamber. *J. Aerosol Sci.* 52: 18–32.

Bhangar, S., Mullen, N.A., Hering, S.V., Kreisberg, N.M. and Nazaroff, W.W. (2011). Ultrafine particle concentrations and exposures in seven residences in northern California. *Indoor Air* 21: 132–144.

Dhaniyala, S., Dubey, P. and Balakrishnan, K. (2011). Air quality in rural India: The role of ultrafine particles from cookstoves. Environmental Manager, Magazine of American Waste and Air Association, pp. 14–18.

Hendriks, E.M. and Ziff, R.M. (1985). Coagulation in a continuously stirred tank reactor. *J. Colloid Interface Sci.* 105: 247–256.

Hussein, T., Korhonen, H., Herrmann, E., Hameri, K., Lehtinen, K.E.J. and Kulmala, M. (2005) Emission rates due to indoor activities: indoor aerosol model development, evaluation, and applications. *Aerosol Sci. Technol.* 39: 1111–1127.

Kittelson, D.B. (1998). Engines and nanoparticles: A review. *J. Aerosol Sci.* 29: 575–588.

Kittelson, D.B. (2001). Recent measurements of nanoparticle emissions from engines, current research on diesel exhaust particles. Japan Association of Aerosol Science and Technology, Tokyo.

Lai, A.C.K. and Nazaroff, W.W. (2000). Modeling indoor particle deposition from Turbulent flow onto smooth surfaces. *J. Aerosol Sci.* 31: 463–476.

Mitra, A.P., Morawska, L., Sharma, C. and Zhang, J. (2002). Chapter two: methodologies for characterization of combustion sources and for quantification of their emissions. *Chemosphere* 49: 903–922.

Mullen, N.A., Bhangar, S., Hering, S.V., Kreisberg, N.M. and Nazaroff, W.W. (2011). Ultrafine particle concentrations and exposures in six elementary school classrooms in northern California. *Indoor Air* 21: 77–87.

Reddy, M.S. and Venkataraman, C. (2002). Inventory of aerosol and sulphur dioxide emissions from India: I - Fossil fuel combustion. *Atmos. Environ*. 36: 677–697.

Wallace, L. and Ott, W. (2011). Personal exposures to ultrafine particles. *J. Exposure Sci. Environ. Epidemiol.* 21: 20–30.

Wallace, L., Emmerich, S.J. and Howard-Reed, C. (2004). Source strengths of ultrafine and fine particles due to cooking with a gas stove. *Environ. Sci. Technol.* 38: 2304–2311.

Wallace, L., Wang, F., Howard-Reed, C. and Persily, A. (2008). Contribution of gas and electric stoves to residential ultrafine particle concentrations between 2 and 64 nm: Size distributions and emission and coagulation rates. *Environ. Sci. Technol.* 42: 8641–8647.

Wolfram Research, Inc. (2005). Mathematica, version 5.2, Champaign, IL.

Received for review, October 9, 2015
Revised, January 4, 2016
Accepted, January 8, 2016